Construction and Control of Massive Hydraulic Micro-actuator-sensor Array

Haihong Zhu, Wayne J. Book

Abstract—**Massive actuator arrays found their applications in robotics, pharmaceutics, aerospace, etc. Compared with electrically and/or pneumatically powered actuator array, hydraulic actuator has the comprehensive advantages of higher force density (i.e. force / actuation area), better controllability, and simpler remote control accessibility. This paper presents approaches to construct and control a massive hydraulic micro actuator array. The massive hydraulic actuator array is originally constructed for project "Digital Clay" (a novel hydraulic actuated human machine interface device) as the tangible human and machine interaction media. A pin-rod planar actuator array is investigated in this work. In this paper, designs of the practical kinematical structure are discussed, proposed control methods for the actuator array are introduced and experiment results are presented.**

I. Introduction

Massive actuator arrays found their applications in robotics[1], pharmaceutics[2], space science and exploration [3] [4], aircrafts [5], virtual reality and human machine interface [6][7][8], etc. A number of actuation systems have been developed to move and position objects or change the shape of the system. Recent techniques applicable for constructing actuation arrays range from air jets [9][10], electromagnetic actuators [11], piezoelectric actuators [12], single-crystal silicon electrostatic actuators [13], thermal-bimorph (bi-material) actuators [14], shape memory alloy [15] to electro-thermal (single-material) actuators [16].

Researchers in Georgia Institute of Technology are working on a novel human computer interface known as Digital Clay [8]. Digital Clay could be described as a "3D monitor" whose pixels can move perpendicularly to the screen to form a morphing surface. (Fig. 1) Users can view, touch and shape the working surface formed by these "pixels". In reality, the "pixels" are the tips of micro hydraulic actuators arranged in a matrix formation. Through the actuator array, Digital Clay provides a 2.5D tangible surface actuated under the control of a computer. The user can shape the surface for the computer to understand, and the computer can command the surface shape for the user to feel and see. The potential applications of Digital Clay cover a wide range from computer aided engineering design, scientific research, medical diagnoses, 3D dynamic mapping, to education.

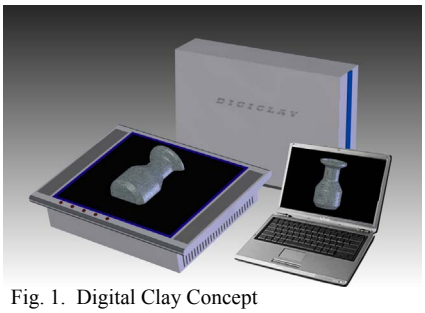

Fig. 1. Digital Clay Concept

The massive micro-actuator array is the key to realize the concept of Digital Clay. To achieve special resolution, the actuator array could consist of a large number of micro/miniature actuators with sensing ability. Furthermore, output maximum force is also an important feature since the surface is to be touched by human user. Hydraulic actuation system is used because, compared with electrical and pneumatic systems, hydraulic actuator has the comprehensive advantages of higher force density (i.e. force / actuation area), better controllability, and simpler remote control accessibility. These advantages are critical to meet the requirements on the actuator array, e.g., small actuator size (ϕ1 ~ ϕ4mm OD), large force output (>1 N / actuator), long stroke (>40 mm), and high density (25 ~ 150 DPI), etc.

In this paper, practical structural designs, displacement sensing technology and control methods for the massive hydraulic micro actuator array are presented.

II. Mechanical Structure of the Actuator Array

A. Single Actuator

Constrained by the requirement on size, it is difficult to find an off-the-shelf hydraulic linear actuator, which prompts the efforts on design a customized actuator. Two solutions have been proposed and studied (Fig.2). Experiments showed that both rubber o-ring and graphite seal can provide excellent seal, but the graphite seal reduces more friction and the stiction. Therefore, solution (a) is accepted. The current actuator in use is composed of graphite piston, glass tube, stainless steel rod, and graphite seals.

A problem associated with the graphite seal is the

Manuscript received Feb 10, 2006. This work is supported by the U.S. National Science Foundation ITR grant IIS-0121663.

Haihong Zhu is with Georgia Institute of Technology, Atlanta, GA 30332 USA (phone: 678-644-6386; e-mail: haihong.zhu@ me.gatech.edu).

Wayne J. Book is with Georgia Institute of Technology, Atlanta, GA 30332 USA (e-mail: wayne.book@me.gatech.edu).

leakage. Though tolerances for piston-bore and rod-seal are as tight as 0.0004 inch, leakage is found around 1 ml/min at 10 PSI deferential pressure (from rod-seal). The leakage through the piston is not measured. Currently, the leakage through the piston is compensated depending on displacement feedback and the leakage from rod-seal is removed by a low vacuum system.

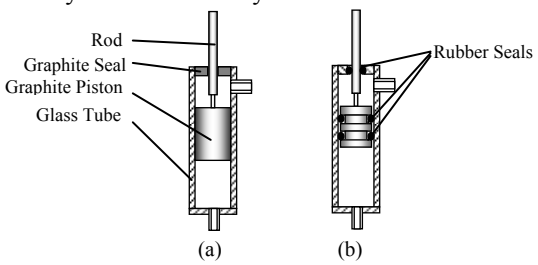

Fig. 2. Alternatives of discrete actuator

B. *Actuator Array*

Constructing a massive hydraulic actuator array by simply stacking actuators together will face obstacles of hydraulic routing and cost on components, e.g., control valves. Solutions provided in following section are for this problem.

1) *Acting Type*

Single acting and double acting are two acting types of fluidics cylinders. In this work, a combination of double and single acting type is used (Fig.3). Upper ports of all actuators are routed together and supplied with a constant pressure for retracting.

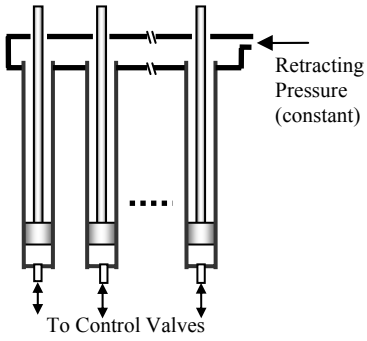

Fig. 3. Constant pressure retracting scheme

Supplying pressure (from control valve) higher than the retracting pressure can extend the actuator and vise versa. The advantage is the simplicity.

2) *Fluidic Matrix Drive*

Per conventional hydraulic actuation strategy, each actuator needs two valves, which implies an N by N actuator array would require $2N^2$ valves and related peripherals. MEMS technology may provide big-orifice micro-valves and solutions on the control hardware ultimately, however miniature solenoid valve is still the most practical choice at this point. Inspiration from LED arrays yields another solution, Fluidic Matrix Drive (FMD), where row and column can be used to identify a given actuator for stimulation.

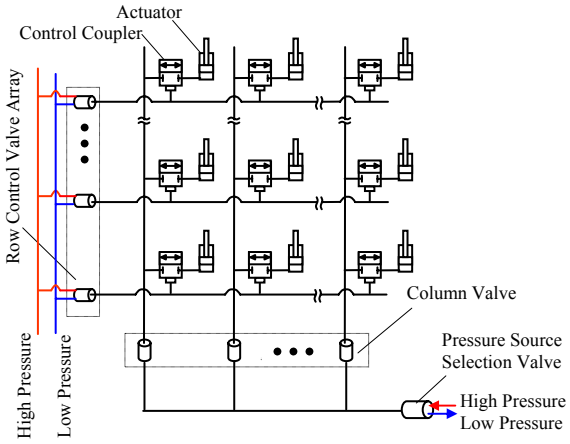

Fig. 4. Fluidic Matrix Drive Concept

The concept and working principle are shown in fig. 4. One set of valves controls the opening of a "control coupler" which is actually a second stage of the fluid valve. Opening a row control solenoid valve connects one entire row of actuators to the column control valves which can then move each actuator in that column. The key is to implement the control coupler compactly, inexpensively and effectively. By refreshing the actuator array row by row, the whole actuator array can be controlled. The actual array refresh methods are not limited to row by row refresh. Three refresh methods will be discussed later in this paper.

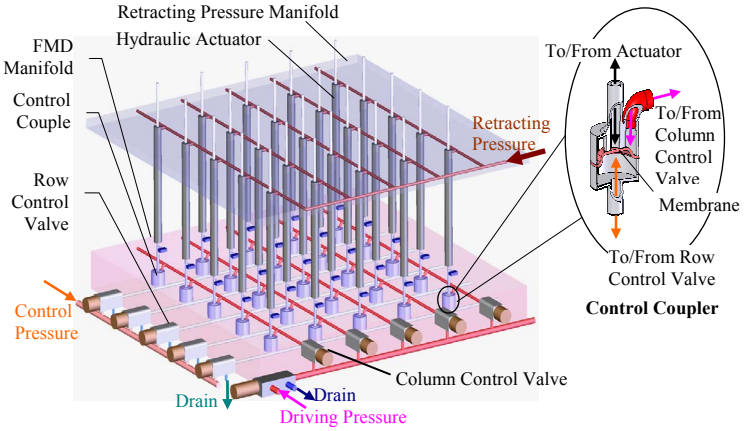

Fig. 5. Structure and Composition of the actuator array (part of the system)

Fig.5 gives a realization scheme of the actuator array. Details on realization of the control coupler are shown on the right of Fig.5. A great reduction of the number of valves is possible however, even with the 5x5 array prototype (will be discussed later) which would require 50 valves when implemented in the previous fashion and only require 10 valves here. The whole array is composed of four major parts: FMD manifold (control coupler included), actuator array, retracting pressure manifold, and control valve array. For the prototype in this work, FMD manifold (with control coupler) and retracting pressure manifold are built at one time using massive and rapid production technology known

as Stereolithography.

III. Capacitively-coupled Position Sensing Technology

Size constraint requires the position sensor for the actuators in this work to be < ϕ1 mm OD with > 50 mm stroke. No such sensor is found on the market, prompting the efforts to design a new displacement sensor. After evaluation of a number of concepts, the capacitively-coupled position sensing technology is conceived and implemented.

A. Working Principle

The Capacitively-coupled Position Transducer (CCPT) is a patent pending, linear displacement sensor technology developed at Georgia Tech and being commercialized by Sentrinsic LLC. Its working principle is depicted in Fig.6. Apply an ac excitation across the resistive film (initially, a Titanium film sputtered outside the glass tube). This will deploy a linear distribution of amplitude of the alternating voltage along the film (Shown under the tube in Fig.6). Coupled through the capacitance between piston and the conductive film, voltage amplitude on the piston reflects the position of the piston. The linearity depends on the uniformity of the film. The initial processing techniques achieve a linear fit with goodness (R2) of 0.9999.

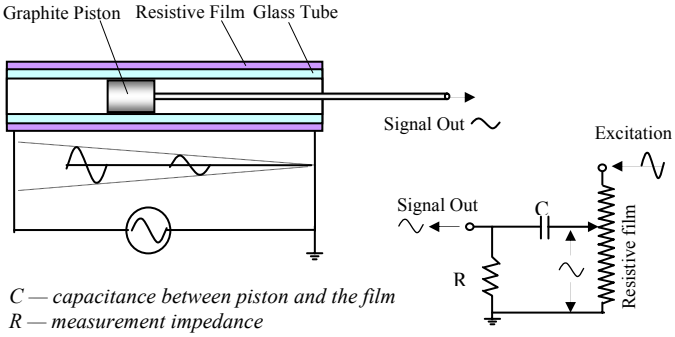

Fig. 6. Capacitively-coupled Position Transducer

B. Signal conditioning

Sinusoidal excitation is commonly used for Linear Variable Deferential Transformer (LVDT). The CCPT sensor also can use a sinusoidal excitation scheme. By comparing the measured signal against the excitation signal, the displacement of the piston can be determined. Initially, a LVDT IC (AD698) was used in this work. However constrained by the cost, a new excitation and signal conditioning technology is designed, which is introduced below.

1) Square-wave excitation signal conditioning

This conditioning scheme is depicted in Fig.7. Instead of applying a sinusoidal excitation voltage, a square waveform is applied across the resistive film. In the simplified scheme depicted in Fig.7, C_1 is the capacitance between the piston the resistive film; C_2 is the capacitance introduced when shielding the signal (to keep the integrity before being processed). C_1 and C_2 are both internal to the sensor. R_m is the impedance of the measurement system.

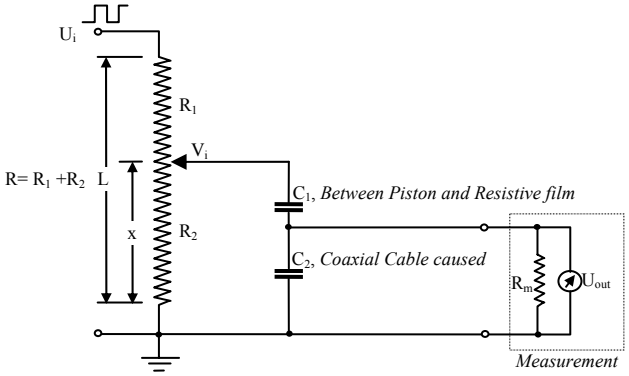

Fig. 7. Square waveform signal conditioning

The output voltage can be found as:

$$U_{out} = \frac{R_2 R_m C_1 s}{R_1 R_2 R_m C_1 C_2 s^2 + (R R_m C + R_1 R_2 C_1) s + R} \cdot U_{in} \qquad (1)$$

$$C = C_1 + C_2; R = R_1 + R_2$$

The output can be further divided into two periods: charging and discharging. Given following values used for the actuator array,

$$R_m = 2 \times 10^8 \Omega, R = 2K\Omega, C_1 = 20\,pf, C_2 = 180\,pF$$

The charging time $<7\times10^{-8}$s (Fig. 8, Matlab), which means signal conditioning bandwidth could be up to 10 MHz.

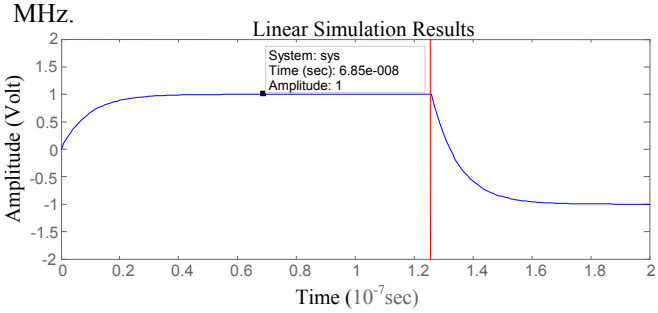

Fig. 8. Charging period Matlab simulation

During discharging, the output can be further simplified as (Rm >>R, using OP Amplifier):

$$U_{out} = \frac{R_2 R_m C_1 s}{R R_m C s + R} \cdot U_{in} = \frac{C_1}{C_1 + C_2} \cdot \frac{x}{L} U_{in} \qquad (2)$$

From the Matlab simulation of the discharging process (Fig. 9), it can be seen that a DAQ sampling frequency higher than 10 KHz can guarantee the drop down < 0.1% of the original signal.

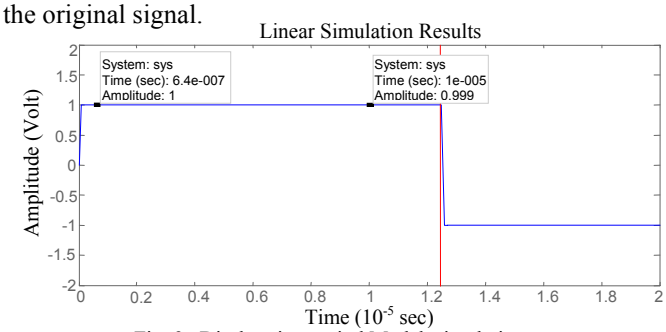

Fig. 9. Discharging period Matlab simulation

The variance of C_1 is small and can be eliminated as shown in Fig.10. In a short period (< 0.01ms), sample the output both with and without capacitor C_3. Then, equation set 3 applies. C_1 usually will not change during above period. Values of C_2, C_3 can be calculated during calibration. Furthermore, C_3 could be any component that can change the measurement impedance (e.g. resistor). Provisional patent on the square wave excitation technology has been filed sponsored by Sentrinsic, LLC.

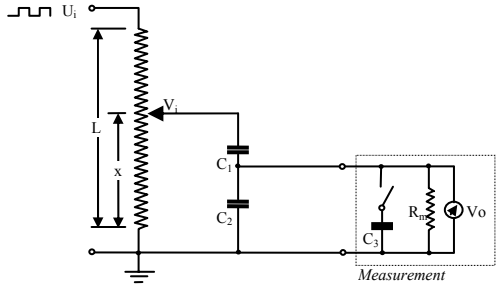

Fig. 10. Eliminate the uncertainty of C_1

$$\begin{cases} U_{out} = \dfrac{C_1}{C_1+C_2}\cdot\dfrac{x}{L}U_{in} \\ U_{out} = \dfrac{C_1}{C_1+C_2+C_3}\cdot\dfrac{x}{L}U_{in} \end{cases} \quad (3)$$

C. *Signal Multiplexing for CCPT Sensor Array*

When dealing with a massive array of signal sources, switching speed and the parameters of non-ideal behavior such as static and dynamic crosstalk are critical especially for the displacement sensor used here (the output is not DC). Crosstalk denotes a situation where the signals on other channels couple with the signal on the channel being measured. There are several forms of crosstalk, all inherent to the multiplexing process, and all worsen as the multiplexing frequency and signal frequencies increase. Two of the tested methods of signal multiplexing for the CCPT sensor array are presented here.

1) *For sine-wave excited signal conditioner (LVDT)*

A scheme used for sine-wave excited signal conditioner is shown in Fig.11. A grounding resistor Rg is utilized to ground the sensor signal before the digital switch.

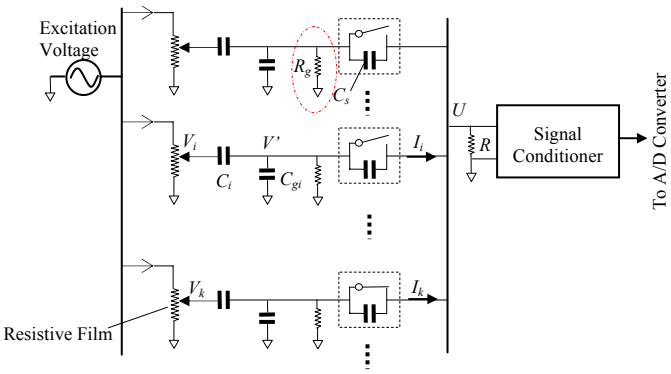

Fig. 11. Multiplexing scheme for sinusoidal wave excited sensor array

The amplitude of the output U can be calculated as (refer to [17] for details):

$$\|U\| = \frac{\sqrt{(e\omega)^2 + (d\omega^2)^2}}{\sqrt{(b\omega)^2 + (c - a\omega^2)^2}} \quad (4)$$

where
$$\begin{cases} a = R_g(C_1+C_2)(C_1+C_2+nC_s) \\ b = (\dfrac{R_g}{R}+2)(C_1+C_2) + (\dfrac{R_g}{R}+n)C_s \\ c = \dfrac{1}{R_g} + \dfrac{1}{R} \\ d = R_g C_1 (C_s \cdot \sum \|V_i\| + (C_1+C_2+C_s)\cdot\|V_k\|) \\ e = C_1\|V_k\| \end{cases}$$

Matlab simulation result is shown in Fig12. Parameters used are according to the real system: 1) number of sensors: 10, 100 and 1000, 2) C_1 = 18pf, 3) C_2 = 30pf, 4) C_s = 0.3pf, and 5) R = 1MΩ and 6) Rg = 20KΩ. The simulation assumes the worst situation that the sensor output of active channel is from 0 ~ 10 volt, while all the inactive channels' outputs are at the maximum value: 10 volt.

It can be seen that for the array with 10, 100 sensors, the measured signals overlap the ideal signal (i.e. not affected by the crosstalk). For the 1000 sensor array, the result at the small voltage (e.g. V_k < 2 V) is not good. However given the fact that the initial working position of sensor can be set at 3 V or more, the problem is easy to solve by sacrificing some of the working range.

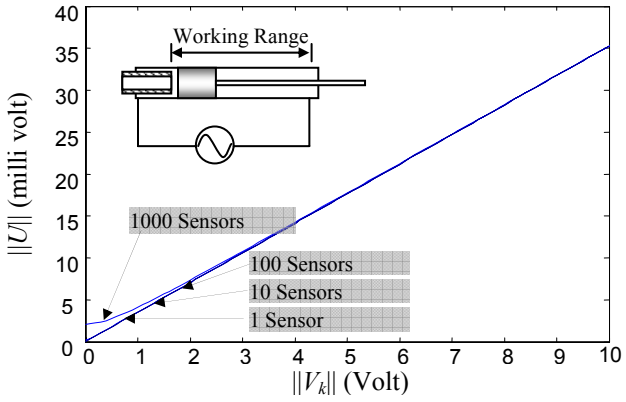

Fig. 12. Results of the Multiplexer

Other solutions are also investigated such as numerically compensate the interference by computer. Using two digital switches (or a Single Throw Double Position switch) in one channel provides another alternative solution. Due to the cost and computational load, these solutions are not implemented.

2) *Signal multiplexing for square-wave excited signal conditioner*

For the square-wave excited situation, signal multiplexing becomes faster, simpler and cheaper. Therefore it is currently applied for the actuator array. The multiplexing scheme is shown in Fig.13.

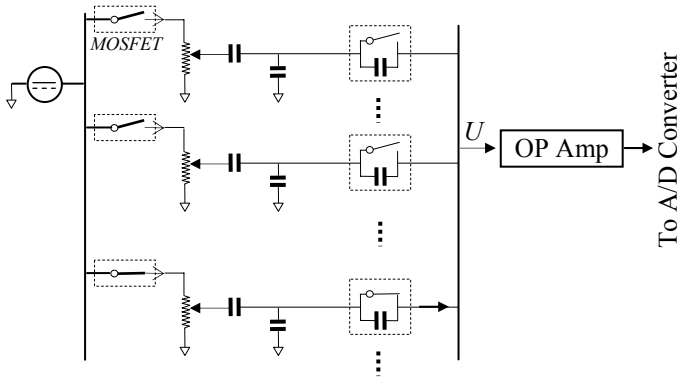

Fig. 13. Multiplexing scheme for square-wave excited sensor array

The differences between this scheme and the scheme in figure 3-6 and corresponding benefits are:

1) dc excitation replaces the ac excitation. The square waveform is generated by simple low cost MOSFET array. It is difficult for ac excitation to use MOSFET, because it will introduce distortion which will affect LVDT signal conditioner (using the excitation as the reference).
2) The inactive sensors are not excited, therefore no interference will present on the signal bus. This not only reduces the interferences caused by the inactive sensors but also allows the using of low cost digital switches or even small size MOSFETs/transistors. The digital switches used in figure 3-6 cost $5/each, while the MOSFETs cost less than $0.1/each.
3) OP Amplifier replaces the LVDT signal conditioner. This reduced the cost more than 50 times and reduced size more than 10 times.
4) No grounding resistors are needed.

IV. CONTROL METHODS FOR FMD BASED HYDRAULIC ACTUATOR ARRAY

Similar to the LED array using Matrix Drive method, Fluidic Matrix Drive based hydraulic actuator array also works on a row and column matching method. Three array refresh methods are discussed in the following sections.

A. Matrix Representation of the Surface Refresh Process

An operation Θ is defined here as an operation subjected to following rule:

$$\mathrm{A}=\begin{bmatrix} a_1 \\ \vdots \\ a_i \\ \vdots \\ a_n \end{bmatrix};\ \text{and}\ \ \mathrm{B}=\begin{bmatrix} b_1 & \cdots & b_j & \cdots & b_n \end{bmatrix};$$

$$\text{Then } \mathrm{A}\Theta\mathrm{B}=\begin{bmatrix} \mathrm{g}(a_1,b_1) & \mathrm{g}(a_1,b_2) & \cdots \\ \mathrm{g}(a_2,b_1) & & \\ \vdots & \ddots & \\ & & \mathrm{g}(a_i,b_j) \end{bmatrix}$$

$$where, a_i = f_1(\delta_i); b_j = f_2(\delta_j);$$

In above definition, A is comprised of the elements that related to the PWM duty cycles δ_i on the row control valve array; B is comprised of the elements that related to the PWM duty cycles δ_j on the column control valve array. g(x, y) depicts the elevation/extension of each actuator in unit time (second). Functions $f_k(\delta_k)$ depend on variables such as pressure drop, discharge coefficient, etc. $f_k(\delta_k)$ will be determined in the future to guarantee g(x, y) = x*y. When the valve is closed $a_i = 0$ and $\delta_i = 0$. When the valve is fully open, $a_i = 1$ and $\delta_i = 100\ \%$. For b_j, same situation applies.

B. One-time Refresh Method

By the one-time refresh method, actuators are controlled to reach their final positions (determined by the surface matrix) row by row and in one step. For example, if the desired final surface matrix is:

$$\mathrm{C}=\begin{bmatrix} 0 & 1 & 2 & 3 & 4 \\ 0 & 0 & 1 & 2 & 3 \\ 0 & 0 & 0 & 1 & 2 \\ 0 & 0 & 0 & 0 & 1 \\ 0 & 0 & 0 & 0 & 0 \end{bmatrix}$$

Assume: maximum speed of actuator is 1 unit/sec; refresh settling time (for valves to stably open and close) is 0.05 sec. The vectors for controlling the valve arrays for the first row refresh are A1 and B1, and the surface matrix is C1.

$$\mathrm{A1}=\begin{bmatrix} 0 & 0 & 0 & 1 & 0 \end{bmatrix}';\quad \mathrm{B1}=\begin{bmatrix} 0 & 0 & 0 & 0 & 1 \end{bmatrix};$$

$$\mathrm{C1}=\mathrm{A1}\Theta\mathrm{B1}*t_1=\begin{bmatrix} 0 & 0 & 0 & 0 & 0 \\ 0 & 0 & 0 & 0 & 0 \\ 0 & 0 & 0 & 0 & 0 \\ 0 & 0 & 0 & 0 & 1 \\ 0 & 0 & 0 & 0 & 0 \end{bmatrix};\ \text{where } t_1 = 1\,\text{sec}$$

For 2nd row:

$$\mathrm{A2}=\begin{bmatrix} 0 & 0 & 1 & 0 & 0 \end{bmatrix}';\quad \mathrm{B2}=\begin{bmatrix} 0 & 0 & 0 & 0.5 & 1 \end{bmatrix};$$

$$\mathrm{C2}=C1+\mathrm{A2}\Theta\mathrm{B2}*t_2=\begin{bmatrix} 0 & 0 & 0 & 0 & 0 \\ 0 & 0 & 0 & 0 & 0 \\ 0 & 0 & 0 & 1 & 2 \\ 0 & 0 & 0 & 0 & 1 \\ 0 & 0 & 0 & 0 & 0 \end{bmatrix};\ \text{where } t_2 = 2\,\text{sec}$$

Similar for 3rd row and 4th row,

$$\mathrm{A3}=\begin{bmatrix} 0 & 1 & 0 & 0 & 0 \end{bmatrix};\quad \mathrm{B3}=\begin{bmatrix} 0 & 0 & 1/3 & 2/3 & 1 \end{bmatrix};$$
$$\mathrm{C3}=C2+A3\Theta B3*t_3,\quad \text{where } t_3 = 3\,\text{sec}$$
$$\mathrm{A4}=\begin{bmatrix} 1 & 0 & 0 & 0 & 0 \end{bmatrix};\quad \mathrm{B4}=\begin{bmatrix} 0 & 0.25 & 0.5 & 0.75 & 1 \end{bmatrix};$$
$$\mathrm{C4}=C3+A4\Theta B4*t_4,\quad \text{where } t_4 = 4\,\text{sec}$$

The total time used is $t_1+t_2+t_3+t_4+4\times$Settling Time (0.05) = 10.2 sec. One-time refresh method is the simplest surface refresh method, but the visual effect is bad (for Digital Clay as a human machine interface) due to obvious discontinuous movement of the pin-rods.

C. Gradual Refresh Method

A solution to make the surface refresh smoother is

gradually achieving the final surface through several intermediate surfaces. The increment of each intermediate surface is a fraction of the final surface. Take the same desired surface in section B as an example. By dividing the final surface matrix into 4 intermediate surfaces as:

$$\begin{bmatrix} 0 & 0 & 0 & 0 & 0 \\ 0 & 0 & 0 & 0 & 0 \\ 0 & 0 & 0 & 0 & 0 \\ 0 & 0 & 0 & 0 & 0 \\ 0 & 0 & 0 & 0 & 0 \end{bmatrix} \Rightarrow \begin{bmatrix} 0 & 1/4 & 1/2 & 3/4 & 1 \\ 0 & 0 & 1/4 & 1/2 & 3/4 \\ 0 & 0 & 0 & 1/4 & 1/2 \\ 0 & 0 & 0 & 0 & 1/4 \\ 0 & 0 & 0 & 0 & 0 \end{bmatrix} \Rightarrow \begin{bmatrix} 0 & 1/2 & 1 & 3/2 & 2 \\ 0 & 0 & 1/2 & 1 & 3/2 \\ 0 & 0 & 0 & 1/2 & 1 \\ 0 & 0 & 0 & 0 & 1/2 \\ 0 & 0 & 0 & 0 & 0 \end{bmatrix}$$

$$\Rightarrow \begin{bmatrix} 0 & 3/4 & 3/2 & 9/4 & 3 \\ 0 & 0 & 3/4 & 3/2 & 9/4 \\ 0 & 0 & 0 & 3/4 & 3/2 \\ 0 & 0 & 0 & 0 & 3/4 \\ 0 & 0 & 0 & 0 & 0 \end{bmatrix} \Rightarrow \begin{bmatrix} 0 & 1 & 2 & 3 & 4 \\ 0 & 0 & 1 & 2 & 3 \\ 0 & 0 & 0 & 1 & 2 \\ 0 & 0 & 0 & 0 & 1 \\ 0 & 0 & 0 & 0 & 0 \end{bmatrix}$$

The time used to realize each intermediate surfaces using one-time refresh method can be found as: 2.7 sec. Therefore the total time for the surface generation is 10.8 sec. The more intermediate surfaces are used, the smother the surface generation process is, but the longer time it takes. The excessive time is spent on the refresh settling processes. For the actuator array constructed in this work, the refresh settling time is around 50~100 ms.

D. Approximation Gradual Refresh Method

One-time refresh method and gradual refresh method are essentially the same: row refresh are processed one after another. For the approximation gradual refresh method, the whole surface may be refreshed at the same time. Take the same desired final surface as in section B. Set the first intermediate surface as:

$$A1 = [1 \quad 3/4 \quad 1/2 \quad 1/4 \quad 0]^T; \quad B1 = [0 \quad 1/4 \quad 1/2 \quad 3/4 \quad 1];$$

$$C1 = A1 \Theta B1 * t_1 = \begin{bmatrix} 0 & 0.500 & 1.00 & 1.500 & 2.0 \\ 0 & 0.375 & 0.75 & 1.125 & 1.5 \\ 0 & 0.250 & 0.50 & 0.750 & 1.0 \\ 0 & 0.125 & 0.25 & 0.375 & 0.5 \\ 0 & 0 & 0 & 0 & 0 \end{bmatrix}; \text{ wher } t_1 = 2 \text{ sec}$$

The second intermediate surface can be:

$$C2 = C - C1 = \begin{bmatrix} 0 & 0 & 0 & 0 & 0 \\ 0 & -0.75 & -0.5 & -0.25 & 0 \\ 0 & -0.50 & -1.0 & -0.5 & 0 \\ 0 & -0.25 & -0.5 & -0.75 & 0 \\ 0 & 0 & 0 & 0 & 0 \end{bmatrix}$$

C2 can be achieved by one time refresh method:

$$\begin{bmatrix} 0 & 0.500 & 1.00 & 1.500 & 2.0 \\ 0 & 0.375 & 0.75 & 1.125 & 1.5 \\ 0 & 0.250 & 0.50 & 0.750 & 1.0 \\ 0 & -0.125 & -0.25 & -0.375 & 0.5 \\ 0 & 0 & 0 & 0 & 0 \end{bmatrix} \Rightarrow \begin{bmatrix} 0 & 0.500 & 1.00 & 1.500 & 2.0 \\ 0 & 0.375 & 0.75 & 1.125 & 1.5 \\ 0 & -0.250 & -0.50 & -0.250 & 1.0 \\ 0 & -0.125 & -0.25 & -0.375 & 0.5 \\ 0 & 0 & 0 & 0 & 0 \end{bmatrix}$$

$$\Rightarrow \begin{bmatrix} 0 & 0.500 & 1.00 & 1.500 & 2.0 \\ 0 & -0.375 & 0.25 & 0.875 & 1.5 \\ 0 & -0.250 & -0.50 & 0.250 & 1.0 \\ 0 & -0.125 & -0.25 & -0.375 & 0.5 \\ 0 & 0 & 0 & 0 & 0 \end{bmatrix}$$

The time used is t_2 = 2.65 s (including the settling time). Finally apply:

$$A2 = [1 \quad 3/4 \quad 1/2 \quad 1/4 \quad 0]^T; \quad B2 = [0 \quad 1/4 \quad 1/2 \quad 3/4 \quad 1];$$

$$C3 = C1 + C2 + A2 \Theta B2 * t_3 = \begin{bmatrix} 0 & 1 & 2 & 3 & 4 \\ 0 & 0 & 1 & 2 & 3 \\ 0 & 0 & 0 & 1 & 2 \\ 0 & 0 & 0 & 0 & 1 \\ 0 & 0 & 0 & 0 & 0 \end{bmatrix}; \text{ where } t_3 = 2 \text{ sec}$$

Therefore, the total time is t_1+t_2+t_3+2×Settling Time (0.05) = 6.75 s, which is much shorter than the other two refresh methods. If (per conventional method) using 50 valves for this application, it also needs 4 seconds to generate the required surface.

The intermediate surfaces used in this method usually are not proportional to the final surface, but the superposition of these intermediate surfaces yields the final surface. By this approach, the total refreshing time can be reduced and a gradually changed surface can be achieved. The problem foreseen in this method is the decomposition of the desired surface matrix into intermediate surface matrices. The solutions to the problem will be left for future research.

V. Experimental Results

At this point, a 5 x 5 array prototype is implemented for testing purpose (Fig.13). The grid size of the array is 5 mm square; each actuator has 4mm OD, 50 mm stroke and 1N maximum force at 20 PSI.

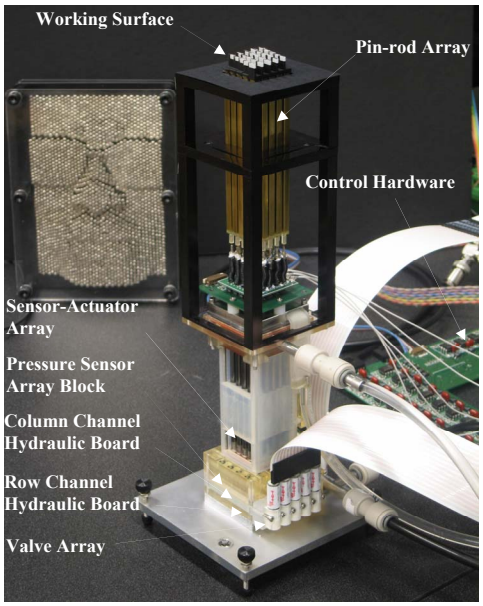

Fig. 13. Digital Clay 5×5 Prototype

A. Surface generation

Surface generation comes closest to capturing the entire purpose of digital clay in a single test. A slanted plane was

generated and the tips of the rods were measured with a camera and processed digitally to verify the locations. Camera measurements are significantly less precise than the position transducer used in the feedback control, but they do provide an independent means of verifying the array positions. As a test, the working surface is commanded to achieve a slanted plane as shown in Fig.14. The commanded and measured elevation matrixes of the working surface given below show less than 0.8 mm error (no filtering, no calibration). Further better results will be given at the final paper.

Commanded surface shape:

$$\begin{bmatrix} 16 & 20 & 24 & 28 & 32 \\ 12 & 16 & 20 & 24 & 28 \\ 8 & 12 & 16 & 20 & 24 \\ 4 & 8 & 12 & 16 & 20 \\ 0 & 4 & 8 & 12 & 16 \end{bmatrix}$$

Detected shape by Machine Vision

$$\begin{bmatrix} 15.6 & 20.4 & 24.3 & 27.7 & 31.2 \\ 11.7 & 16.5 & 20.8 & 23.8 & 28.7 \\ 7.8 & 12.1 & 16.0 & 20.5 & 24.6 \\ 4.3 & 8.7 & 11.7 & 16.8 & 19.5 \\ 0 & 4.3 & 8.2 & 12.1 & 16.5 \end{bmatrix}$$

Fig. 14. Slanted plane formed and measured by camera.

To test the velocity control ability of the proposed PWM flow control method, a single rod is commanded to track a sinusoidal trajectory. The measured results are shown in Fig.15. The solid line is the commanded trajectory and the hollow dots represent the measured displacement.

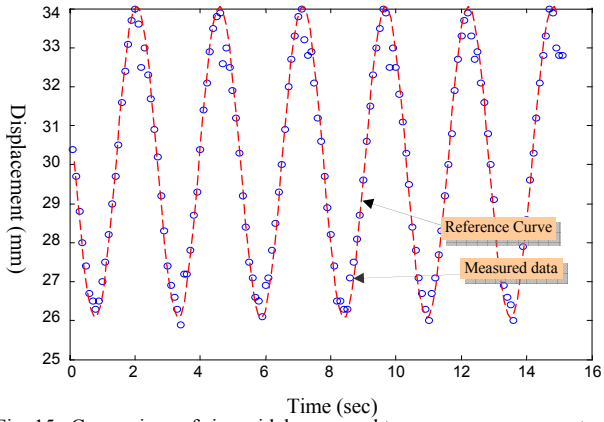

Fig. 15. Comparison of sinusoidal command to camera measurements of a single cell's motion.

VI. Future Work

Above design approaches are aimed at a massive actuator array. However, further work is required to reduce the cost and optimize the structure in order to build an array consisting of more actuators. The peripheral devices such as pressure source, control hardware and high level user application interface are still large in size and rough. Future work is carried out on the optimization of hardware such as compact peripheral support devices and the development of efficient and comprehensive control algorithms such as the approximation gradual refresh method.

VII. Conclusions

In this paper, approaches to construct and control a massive micro hydraulic actuator array in a scaleable style are presented. Specifically, at the component level, a micro hydraulic actuator constructed using graphite and glass tube is introduced; at the array level, a fluidic matrix drive technology is presented; for displacement feedback, a new displacement sensing technology, the CCPT technology is presented along with its signal conditioning methods and related signal multiplexing technology. Based on the fluid matrix drive, three control methods are presented, two of them are implemented and the third one needs further investigation. Finally, the actuator array and control method are validated through experimental results on a 5 by 5 actuator array prototype.

Acknowledgment

The assistance of the co-investigators (Mark Allen, Ari Glezer, John Goldthwaite, David Rosen, Jarek Rossignac, Imme Ebert-Uphoff) and their colleagues and graduate students in the Schools of Mechanical Engineering and Electrical and Computer Engineering, and the College of Computing is gratefully acknowledged.

References

[1] P. E. Kladitis, V.M. Bright, K. F. Harsh and Y. C. Lee, Prototype microrobots for micro positioning in a manufacturing process and micro unmanned vehicles, "Proc. of IEEE MEMS '99, pp. 570-575, 1999.

[2] A. B. Frazier, B. K. Gale, and I. Papautsky, "Micromachined metallic pipettes and bioanalysis systems," in Proc. International Symposium on Mechatronics and Human Science (MHS '97), Nagoya, Japan, Oct. 5-8, 1997, pp. 5-12 (8 pages).

[3] Cabuz, C., Cabuz, E.I., Rolfer, T., Herb, W., Zook, D. "Mesoscopic sampler based on 3d array of electrostatically activated diaphragms," 10th Int. Conf. on Solid-State Sensors and Actuators, Transducers'99, June 7-12, 1999, Sendai, Japan

[4] US-Patent 5,836,750, Electro-statically Actuated Mesopump Having a Plurality of Elementary Cells (C. Cabuz)

[5] Terry, M. L.; Reiter, J.; Boehringer, K. F.; Suh, J. W.; Kovacs, G. J. A docking system for microsatellites based on MEMS actuator arrays. Smart Materials and Structures. 2001; 10: 1176-1184.

[6] H. Iwata, H. Yano, F. Nakaizumi, and R. Kawamura, "Project FEELEX: Adding haptic surface to graphics," in Proceedings of SIGGRAPH2001, 2001

[7] H. Raffle, M. W. Jachim amd J. Tichenor: "Super Cilia Skin: An Interactive Membrane," Conference on Human Factors in Computing Systems, April, 2003

[8] Haihong Zhu and Wayne J. Book, "Practical Structure Design and Control for Digital Clay", 2004 ASME International Mechanical Engineering Congress and Exhibition, vol., p. 1051, 2004

[9] Pister K S J, Fearing R and Howe R 1990 A planar air levitated electrostatic actuator system Proc. IEEE 5th Workshop on Micro Electro Mechanical Systems (Napa Valley, CA, Feb. 1990) pp 67–71

[10] Mita Y, Konishi S and Fujita H 1997 Two-dimensional micro-conveyance system with through holes for electrical and fluidic interconnection Transducers '97 Dig. 9th Int. Conf. on Solid-State Sensors and Actuators (IEEE) (Chicago, IL, June 1997) vol 1 pp 37–40

[11] Liu C, Tsai T, Tai Y-C, Liu W, Will P and Ho C-M 1995 A micromachined permalloy magnetic actuator array for micro robotics assembly systems Transducers '95 Dig. 8th Int. Conf. on Solid-State

Sensors and Actuators/Eurosensors IX (IEEE) (Stockholm, Sweden, June 1995) vol 1 pp 328–31
[12] Furihata T, Hirano T and Fujita H 1991 Array-driven ultrasonic microactuators Transducers '91 Dig. 6th Int. Conf. on Solid State Sensors and Actuators (IEEE) (San Francisco, CA, June 1991) pp 1056–9
[13] B¨ohringer K-F, Donald B R and MacDonald N C 1996 Single-crystal silicon actuator arrays for micro manipulation tasks Proc. IEEE 9th Workshop on Micro Electro Mechanical Systems (MEMS) (San Diego, CA, Feb. 1996) pp 7–12
[14] Takeshima N and Fujita H 1991 Polyimide bimorph actuators for a ciliary motion system ASME WAM, Symp. on Micromech. Sensors, Actuators, and Systems DSC vol 32 pp 203–9
[15] Nakatani, Kajimoto, Sekiguchi, Kawakami, Tachi, "3D Form Display with Shape Memory Alloy, " in Proc. of International Conference on Artificial Reality and Telexistence 2003. (ICAT 2003)
[16] Ebefors T, Mattsson J U, K`elvesten E and Stemme G 1999 A robust micro conveyor realized by arrayed polyimide joint actuators Proc. IEEE 12th Workshop on Micro Electro Mechanical Systems (MEMS) (Orlando, FL, Jan. 1999) pp 576–81
[17] H. Zhu, W. Book, "Embedding and Multiplexing Large Scale Sensor Arrays for Digital Clay", Proceeding of ASME International mechanical Engineering Congress and Exposition, Orlando, 2005.